Simple Ethers as Models of Sugar Molecules in Calculations of Vertical Excitation Energies of DNA and RNA Nucleosides

Saman Alavi

Steacie Institute for Molecular Sciences, National Research Council of Canada, Ottawa, Ontario K1A 0R6 Canada

Received: April 29, 2005; In Final Form: July 11, 2005

The ribose and deoxyribose molecules of RNA and DNA nucleosides are substituted with simple model compounds 1-methoxy-2-ethanol and 1-methoxypropane to mimic the effect of binding to sugars on the vertical excitation energies of purine and pyrimidine bases. The (*R*)-1-methoxy-2-ethanol, $CH_3OC^*HCH_2OH$, for model ribose nucleosides and (*R*)-1-methoxypropane, $CH_3OC^*HC_2H_5$, for model deoxyribose nucleosides have minimal structural characteristics of ribose and deoxyribose molecules when attached to nucleic acid purine and pyrimidine bases. The bases are attached to the C1 carbon atom designated by the asterisk. The vertical excitation energies of these model nucleosides are calculated with the time-dependent density functional theory method at the B3LYP level with 6-311++G(d,p) and aug-cc-pVDZ basis sets. The attachment of the ether molecules qualitatively and quantitatively modifies the excited state energy levels of the model nucleosides when compared to the free bases. These changes can affect the deexcitation mechanisms for photoexcited nucleosides.

1. Introduction

The excited electronic state energy levels[1−5] and dynamics[1,6−11] of purine and pyrimidine bases determine the photoreactivity of DNA and RNA molecules. The photostability of DNA prevents damage to nucleic acids from solar UV radiation and is due to the ultrafast radiationless decay of electronically excited nucleic acid bases. The vertical excitation energies and state assignments of singlet excited states of the isolated purine and pyrimidine base pairs are well-known.[1,2] The lowest energy nπ^* or $\pi\pi^*$ transitions are localized on the aromatic ring systems of the bases and can form conical intersections with the ground electronic state, leading to ultrafast decay.[6,7,9] In isolated bases, low-lying $\pi\sigma^*$ transitions from the pyrimidine N1−H1 and purine N9−H9 bonds can also affect the excited state relaxation dynamics of the base.[10] In nucleosides these N−H bonds are replaced by N−C glycosidic bonds which removes the low-lying $\pi\sigma^*$ transitions for the N1 or N9 σ-bonds.[6,7,10]

The uridine and deoxythymidine nucleosides are shown in Figure 1. In ribose nucleosides the furanose oxygen and the ring C2 hydroxyl oxygen are in proximity to the base, while in the deoxyribose nucleosides the single furanose ether oxygen is in close proximity to the base. These oxygen atoms can be the source of new low-lying nπ^* transitions in the nucleosides that may affect the relaxation dynamics of the bases. Nucleosides are observed[1] to have faster excited state decay rates than free bases. Due to their large size, to the best of our knowledge, high-level theoretical calculations on the excited state structures of the nucleoside molecules have not been performed.

Recently, Zhang, Peritz, and Meggers[11] synthesized DNA and RNA analogues using a three-carbon propylene glycol phosphodiester backbone. The resulting glycol nucleic acid (GNA) molecules form Watson−Crick base pairs and helical structures similar to DNA. These experiments provide motivation for choosing minimal sugar analogues for computational studies of nucleosides. Two ethers, 1-methoxy-2-ethanol and 1-methoxypropane, are proposed to mimic the structure of ribose and deoxyribose, respectively. Structures of the model (*R*)-1-methoxy-2-ethanol "nucleosides" of uracil, cytosine, adenine, and guanine are shown in Figure 2, and model (*R*)-1-methoxypropane "nucleosides" with thymine, cytosine, adenine, and guanine are shown in Figure 3. The bonding and geometric configuration of the sugar analogues are optimized to mimic the real ribose and deoxyribose nucleosides shown in Figure 1 as closely as possible.

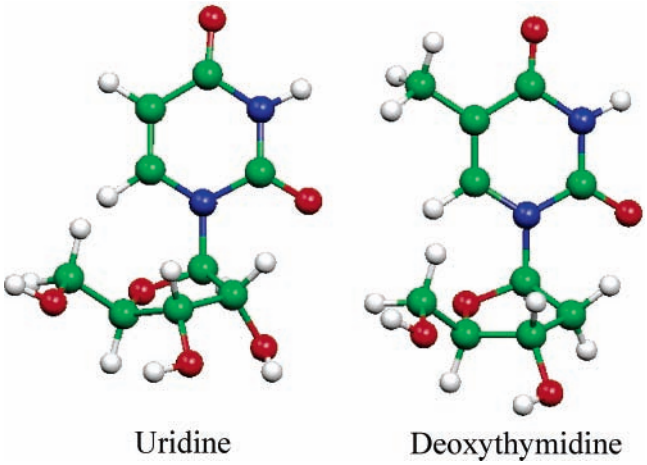

Figure 1. Structures of uridine and deoxythymidine nucleosides. The ribose nucleosides have an OH group attached to the C2 ring carbon atom, which may introduce low-lying nπ^* transitions. The other hydroxyl oxygen atoms are farther from the purine and pyrimidine bases. Nitrogen atoms are shown by blue spheres, oxygen atoms by red spheres, hydrogen atoms by white spheres, and carbon atoms by green spheres.

In this work, the first four vertical excitation energies for the isolated bases and model nucleosides are determined with electronic structure methods. The goal is to determine how binding to the ether molecules will change the electronic excited

10.1021/jp052238l CCC: $30.25 © 2005 American Chemical Society
Published on Web 09/29/2005

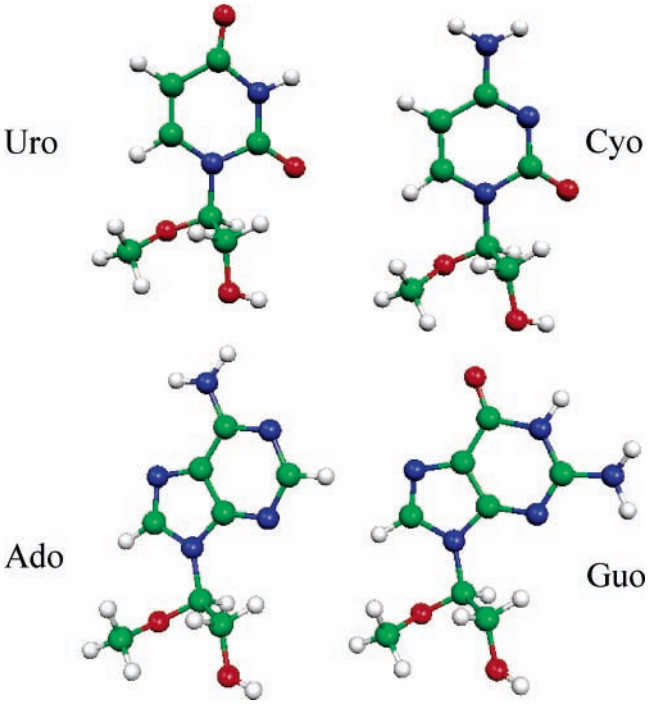

Figure 2. Structures of model "nucleosides" of uracil, cytosine, adenine, and guanine with (*R*)-1-methoxy-2-ethanol. The C1 carbon has an *R* configuration. The ether and hydroxyl oxygen atoms in the model compounds have geometric configurations similar to the nucleosides shown in Figure 1. The color coding of the atoms is given in Figure 1.

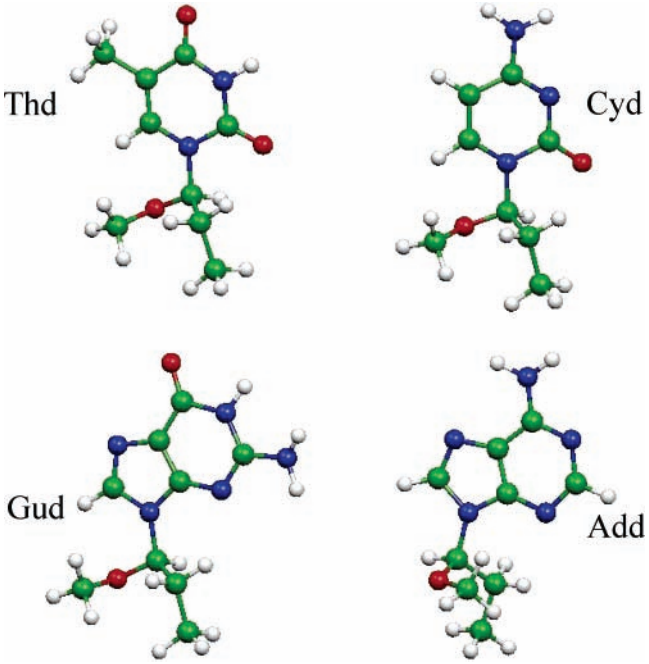

Figure 3. Structures of model "nucleosides" of thymine, cytosine, guanine, and adenine with (*R*)-1-methoxypropane. The model adenine compound optimized to a configuration that is not similar to the deoxyadenosine structure of the nucleoside and is not included in the excited electronic state calculations. The color coding of the atoms is described in Figure 1.

state structures of the bases. These changes could have an effect on the deexcitation mechanisms of nucleosides.

2. Computational Methods

Optimized structures of the isolated bases, 1-methoxy-2-ethanol model nucleosides, and 1-methoxypropane model nucleosides with uracil, thymine, cytosine, adenine, and guanine bases were determined with the Gaussian 98 suite of programs.[12] Density functional theory[13] with the B3LYP Becke[14] hybrid Hartree−Fock nonlocal modification of the Lee, Yang, and Parr functional[15] and the 6-311++(d,p) basis set were used for structural optimizations. Unlike the relatively rigid ring structures of the ribose sugars, the model acyclic ethers are flexible and can take different conformations. Only conformers that give local positioning of ether atoms similar to ribose nucleosides are accepted. The initial input geometries for optimization were chosen to give configurations of the oxygen atoms corresponding to the furanose oxygen of ribose and deoxyribose shown in Figure 1. During the optimization, structures that relaxed to configurations not compatible with the ribose systems were rejected. All (*R*)-1-methoxy-2-ethanol nucleoside model compounds optimize to structures with configurations similar to nucleosides. The optimized structures are shown in Figure 2. The optimized structure of the model deoxyribose nucleoside molecules are given in Figure 3. The (*R*)-1-adenine-1-methoxypropane compound relaxes to a configuration that is not similar to the deoxyribose nucleoside, and this model compound is not included in the analysis of the excited electronic levels. Normal-mode analysis was performed on each optimized structure to verify that it is a stable ground state structure.

Vertical excitation energies were determined with the time-dependent density functional theory (TDDFT)[16,17] method at the B3LYP level with the 6-311++G(d,p) basis set. The TDDFT method gives the proper spectroscopic ordering of excited states for the bases,[1,2] and this basis set is known to give converged results for relatively low-lying excited states.[2] The first four vertical excitation energies for each molecule are determined along with the oscillator strengths of the transition. In addition, the transitions are characterized by giving the major contributing states to each excitation. To verify the accuracy of the vertical excitation energies at the B3LYP/6-311++G(d,p) level, a second set of calculations were performed using the same structures but with the augmented correlation-consistent polarized double-ζ basis set of Dunning[18] [B3LYP/aug-cc-pVDZ//B3LYP/6-311++G(d,p)]. The correlation-consistent basis sets give more reliable results for features of the excited state levels.[18,19] Where possible, the calculated results are compared to experimental data.

3. Results

3.1. Isolated Bases. The vertical excitation energies for the isolated purine and pyrimidine bases are given in Table 1, along with the electronic states that make the greatest contribution to each transition. In assigning states to the transitions, the highest occupied molecular orbital (HOMO) and lowest unoccupied molecular orbital (LUMO) states are used as reference and are shown with "H" and "L", respectively. The nature of the nπ* transitions are further characterized by showing the atoms where the nonbonding orbital is primarily localized. The primary locations of the σ* excitations are also given. The first four excitation energies of the isolated and solvated pyrimidine bases are shown in Figure 4, and the corresponding results for the purine bases are shown in Figure 5. Calculated values with both 6-311++G(d,p) and aug-cc-pVDZ basis sets are connected by lines and are in good agreement. The 6-311++G(d,p) vertical excitation energies are systematically higher than the aug-cc-pVDZ results.

Some experimental[1,2] and calculated[1,2] vertical excitation energies of the isolated bases are also given in Table 1. Only $\pi\pi$* transitions with large oscillator strengths are experimentally detected. The agreement between the experimental vertical

TABLE 1: First Four Vertical Excitation Energies (eV) along with Their Assignments and Oscillator Strengths (in Parentheses) for Isolated Pyrimidine and Purine Bases Calculated with the TDDFT Method

base	transition[a]	energy calcd[a]	energy calcd[b]	energy calcd	energy expt[c]
Ur	$n_{H-1}(O)\pi^*_L$	4.68 (0.000)	4.65 (0.000)	4.67,[d] 4.61[e]	
	$\pi_H\pi^*_L$	5.18 (0.132)	5.13 (0.122)	5.17,[d] 5.44[e]	4.6−5.1
	$\pi_H\sigma^*_{L+1}$(N1−H1)	5.69 (0.002)	5.62 (0.002)	5.69,[d] 5.83[e]	
	$n_{H-3}(O)\pi^*_L - n_{H-1}(O)\pi^*_{L+2}$	5.80 (0.000)	5.76 (0.000)	5.80,[d] 5.95[e]	5.8−6.1
Th	$n_{H-1}(O)\pi^*_L$	4.75 (0.000)	4.73 (0.000)	4.71[d]	
	$\pi_H\pi^*_L$	4.99 (0.137)	4.94 (0.128)	4.95[d]	4.5−4.9
	$\pi_H\sigma^*_{L+1}$(N1−H1)	5.45 (0.000)	5.39 (0.000)	5.44[d]	
	$n_{H-3}(O)\pi^*_L$	5.86 (0.000)	5.82 (0.000)	5.82[d]	
Cy	$\pi_H\pi^*_L$	4.64 (0.043)	4.62 (0.043)	4.63,[d] 4.50[f]	4.5−4.6
	$n_{H-1}(O)\pi^*_L$	4.77 (0.001)	4.75 (0.001)	4.73,[d] 4.88[f]	
	$n_{H-3}(N)\pi^*_L$	5.11 (0.001)	5.12 (0.003)	5.11,[d] 5.23[f]	
	$\pi_H\sigma^*_{L+1}$(N4−H4)	5.23 (0.004)	5.17 (0.005)	5.28[d]	
Ad	$n_{H-1}(N)\pi^*_L$	4.93 (0.001)	4.91 (0.000)	4.88,[d] 5.01[g]	
	$\pi_H\pi^*_L$	4.99 (0.204)	4.95 (0.201)	4.98,[d] 5.04[g]	4.6−4.9
	$\pi_H\sigma^*_{L+1}$(N9−H9)	5.23 (0.006)	5.14 (0.007)	5.28,[d] 5.31[g]	
	$\pi_H\pi^*_{L+2} - \pi_{H-2}\pi^*_L$	5.25 (0.042)	5.22 (0.039)	5.21,[d] 4.90[g]	4.3−4.6
Gu	$\pi_H\pi^*_L$	4.60 (0.021)	4.53 (0.016)	4.67[d]	
	$\pi_H\pi^*_{L+1}$	4.87 (0.135)	4.83 (0.118)	4.88[d]	4.4−4.6
	$\pi_H\sigma^*_{L+3}$(N9−H9)	5.05 (0.007)	4.98 (0.009)	5.08[d]	
	$\pi_H\pi^*_{L+2}$	5.21 (0.231)	5.16 (0.239)	5.18[d]	4.8−5.1

[a] Present work, calculated at the B3LYP/6-311++G(d,p) level. [b] Present work, calculated at the B3LYP/aug-cc-pVDZ level. [c] From multiple experimental sources. For original experimental papers, see Shukla and Leszczynski, ref 2. [d] From MP2/6-311G(d,p) optimized geometric structures using the TDDFT method at the B3LYP/6−311(5+,5+)G(df,pd) level. See Shukla and Leszczynski, ref 2. [e] From DFT/MRCI calculations with the TZVPP+Ryd basis. See Marian et al., ref 6. [f] From CASPT2/6-31** calculations. See Merchàn and Serrano-Andrès, ref 7. [g] From DFT/MRCI calculations with the TZVPP+Ryd basis. See Marian, ref 9.

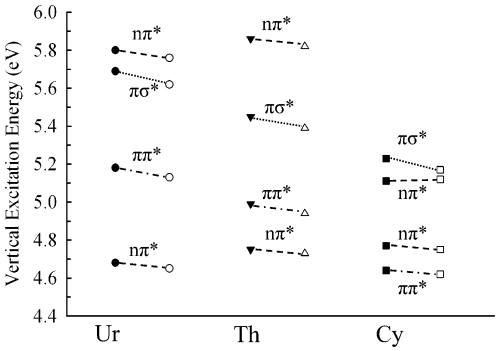

Figure 4. Vertical excitation energies of isolated pyrimidine bases determined at the B3LYP/6-311++G(d,p) (filled symbols) and B3LYP/aug-cc-pVDZ levels (open symbols). Correlations of excited state transitions are shown by connecting the states with lines. Dashed lines correspond to correlations of nπ^* transitions, dashed−dotted lines correspond to correlations among $\pi\pi^*$ transitions, and dotted lines correspond to correlations among $\pi\sigma^*$ transitions. More details of the nature of the transitions are given in Table 1.

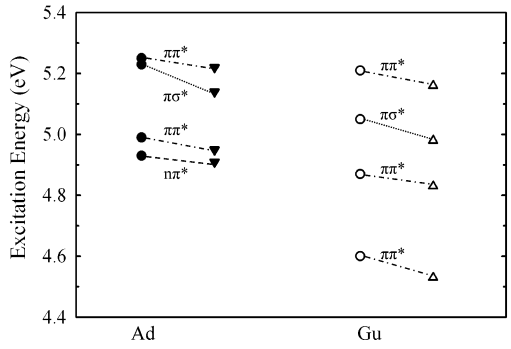

Figure 5. Vertical excitation energies of isolated purine bases determined at the B3LYP/6-311++G(d,p) (circles) and B3LYP/aug-cc-pVDZ levels (triangles). Correlations of excited state transitions are shown by connecting the states with lines. Correlations among nπ^* transitions (dashed lines), $\pi\pi^*$ transitions (dashed−dotted lines), and $\pi\sigma^*$ transitions (dotted lines) are also shown. Further details are given in Table 1.

excitation energies and the results of the present calculations is generally good and within the errors of the methodologies for calculating excited state energies. The state assignments are also consistent with previous TDDFT theoretical calculations.[1,2] The results of DFT multireference configuration interaction (DFT/MRCI) calculations for the vertical excitation energies of uracil[6] and adenine[9] are also given in Table 1. The vertical excitation energies predicted by the MRCI method are somewhat higher than the present TDDFT calculations. Although experimentally observed $\pi\pi^*$ vertical transition energies cannot distinguish between the TDDFT and MRCI results, in the case of uracil, the agreement of the TDDFT results with experiment seems somewhat better.

It is interesting to note that the TDDFT and DFT/MRCI give different orderings of the excited states for adenine. The MRCI method predicts the lowest excitation to be a low-oscillator-strength $\pi\pi^*$ transition, whereas the TDDFT (as well as CASPT2[9]) calculations predict the lowest-lying transition to be nπ^*.

3.2. Model Ribose-like Nucleosides. The first four excitation energies of the model 1-methoxy-2-ethanol derivatives of bases are given in Table 2 and shown in Figures 6−10. The isolated base (X) excited state levels are shown along with the levels of the ribose-like model nucleosides (Xo), at both the 6-311++G(d,p) and aug-cc-pVDZ levels. Correlations with the isolated base states are indicated by lines. As in the case of isolated bases, the 6-311++G(d,p) vertical excitation energies for model nucleosides are systematically higher than the corresponding aug-cc-pVDZ values. In the model nucleosides, the low-lying $\pi\sigma^*$ NH transitions are eliminated since the purine N9−H9 and pyrimidine N1−H1 bonds are replaced by "glycosidic" N−C bonds. The results in Table 2 show that the oxygen atom of the OH group provides a low-lying $\pi\sigma^*$ transition in uracil, thymine, and adenine. Another change in excited state levels is that the higher nπ^* transitions for the Xo species mix in contributions from the ether oxygen and are not exclusively localized on the aromatic ring O and N atoms. These transitions may open new channels for the excited electronic state relaxations.

TABLE 2: First Four Vertical Excitation Energies (eV) and Oscillator Strengths (in Parentheses) along with Their Assignments for Model (*R*)-1-Methoxy-2-ethanol Nucleosides

model nucleoside	transition	energy 6-311++G(d,p)	transition	energy aug-cc-pV DZ
Uro	$n_{H-1}(O)\pi^*_L$	4.71 (0.001)	$n_{H-1}(O)\pi^*_L$	4.68 (0.001)
	$\pi_H\pi^*_L$	5.01 (0.189)	$\pi_H\pi^*_L$	4.96 (0.179)
	$n_{H-2}(M)\pi^*_L + n_{H-3}(M)\pi^*_L$[a]	5.74 (0.004)	$n_{H-2}(M)\pi^*_L + n_{H-3}(M)\pi^*_L$[a]	5.71 (0.004)
	$\pi_H\sigma^*_{L+1}(O-H)$	5.83 (0.010)	$\pi_H\sigma^*_{L+1}(O-H)$	5.75 (0.010)
Tho	$n_{H-1}(O)\pi^*_L$	4.76 (0.010)	$n_{H-1}(O)\pi^*_L$	4.74 (0.017)
	$\pi_H\pi^*_L$	4.86 (0.193)	$\pi_H\pi^*_L$	4.82 (0.178)
	$\pi_H\sigma_{L+1}{}^*(O-H)$	5.57 (0.004)	$\pi_H\sigma_{L+1}{}^*(O-H)$	5.49 (0.003)
	$\pi_H\sigma^*_{L+2}$	5.79 (0.004)	$\pi_H\sigma^*_{L+2}$	5.71 (0.002)
Cyo	$\pi_H\pi^*_L$	4.65 (0.092)	$\pi_H\pi^*_L$	4.62 (0.094)
	$n_{H-1}(M)\pi^*_L - n_{H-2}(O)\pi^*_L$[a]	4.85 (0.002)	$n_{H-1}(M)\pi^*_L - n_{H-2}(O)\pi^*_L$[a]	4.84 (0.002)
	$n_{H-3}(N)\pi^*_L$	5.20 (0.001)	$\pi_H\sigma^*_{L+1} - n_{H-3}(N)\pi^*_L$	5.20 (0.009)
	$\pi_H\sigma^*_{L+1}(C5-H5)$	5.29 (0.005)	$\pi_H\sigma^*_{L+1} + n_{H-3}(N)\pi^*_L$	5.22 (0.005)
Ado	$\pi_H\pi^*_L$	4.92 (0.179)	$\pi_H\pi^*_L$	4.90 (0.188)
	$n_{H-1}(N)\pi^*_L$	4.95 (0.030)	$n_{H-1}(N)\pi^*_L$	4.93 (0.020)
	$\pi_H\pi^*_{L+2} - \pi_H\sigma^*_{L+1}$	5.17 (0.054)	$\pi_H\pi^*_{L+2} + \pi_H\sigma^*_{L+1}$	5.13 (0.045)
	$\pi_H\sigma^*_{L+3} + \pi_H\sigma^*_{L+1}(OH)$	5.33 (0.012)	$\pi_H\sigma^*_{L+3}(OH)$	5.24 (0.019)
Guo	$\pi_H\pi^*_L$	4.47 (0.016)	$\pi_H\pi^*_L$	4.41 (0.012)
	$\pi_H\pi^*_{L+1}$	4.76 (0.125)	$\pi_H\pi^*_{L+1}$	4.72 (0.112)
	$\pi_H\pi^*_{L+2}$	4.92 (0.027)	$\pi_H\pi^*_{L+3}$	4.86 (0.028)
	$\pi_H\pi^*_{L+3}$	5.15 (0.182)	$n_{H-1}(O)\pi^*_{L+1} + n_{H-1}(O)\pi^*_{L+3}$	5.10 (0.183)

[a] A mixed nonbonding state with contributions from the ring O and N atoms as well as the ether O atom.

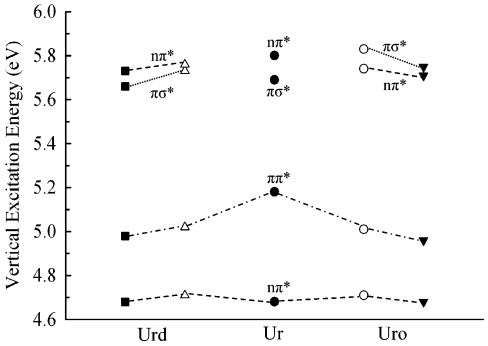

Figure 6. Vertical excitation energies of isolated uracil (Ur), model ribose nucleoside (Uro), and model deoxyribose nucleoside (Urd). Correlations of excited state transitions are shown with lines. Calculations for Uro and Urd at the B3LYP/6-311++G(d,p) level are shown with open symbols, and those at the B3LYP/aug-cc-pVDZ level are shown with filled symbols. Further details of the nature of the transitions are given in Tables 2 and 3.

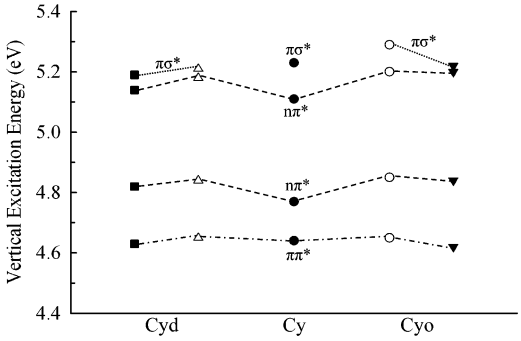

Figure 8. Vertical excitation energies of isolated cytosine (Cy), model ribose nucleoside (Cyo), and model deoxyribose nucleoside (Cyd). Correlations of excited state transitions are shown with lines. Calculations for Cyo and Cyd at the B3LYP/6-311++G(d,p) level are shown with open symbols, and those at the B3LYP/aug-cc-pVDZ level are shown with filled symbols. Further details of the nature of the transitions are given in Tables 2 and 3.

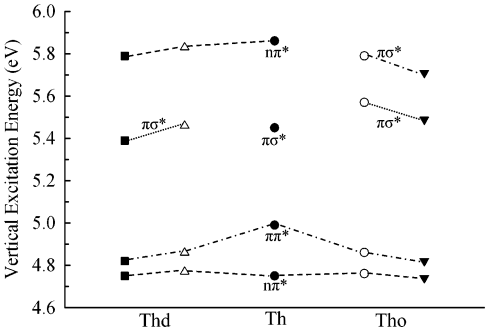

Figure 7. Vertical excitation energies of isolated thymine (Th), model ribose nucleoside (Tho), and model deoxyribose nucleoside (Thd). Correlations of excited state transitions are shown with lines. Calculations for Tho and Thd at the B3LYP/6-311++G(d,p) level are shown with open symbols, and those at the B3LYP/aug-cc-pVDZ level are shown with filled symbols. Further details of the nature of the transitions are given in Tables 2 and 3.

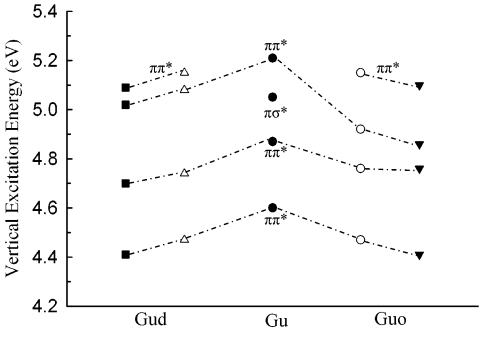

Figure 9. Vertical excitation energies of isolated guanine (Gu), model ribose nucleoside (Guo), and model deoxyribose nucleoside (Gud). Correlations of excited state transitions are shown with lines. Calculations for Guo and Gud at the B3LYP/6-311++G(d,p) level are shown with open symbols, and those at the B3LYP/aug-cc-pVDZ level are shown with filled symbols. Further details of the nature of the transitions are given in Tables 2 and 3.

Except in the case of adenine, the ordering of the first two excited state levels of the spectra of the model nucleosides are unchanged compared to those of the free bases. The vertical excitation energy of the lowest $\pi\pi^*$ transitions are generally red shifted as a result of bonding to the model nucleoside.

3.3. Model Deoxyribose-like Nucleosides. The first four excitation energies of the model 1-methoxypropane derivatives with the bases are given in Table 3 and shown in Figures 6−9. For the isolated base X, the deoxyribose-like model nucleosides are shown as Xd. As in the case of the ribose-like model

TABLE 3: First Four Vertical Excitation Energies (eV) along with Their Assignments and Oscillator Strengths (in Parentheses) for Model (*R*)-1-Methyoxypropane Nucleosides

model nucleoside	transition	energy	transition	energy
Urd	$n_{H-1}(O)\pi^*_L$	4.71 (0.000)	$n_{H-1}(O)\pi^*_L$	4.69 (0.002)
	$\pi_H\pi^*_L$	5.02 (0.200)	$\pi_H\pi^*_L$	4.98 (0.190)
	$\pi_H\sigma^*_{L+3}(CH_3)$	5.73 (0.009)	$\pi_H\sigma^*_{L+3}(CH_3)$	5.66 (0.009)
	$n_{H-3}(M)\pi^*_L$	5.76 (0.002)	$n_{H-3}(M)\pi^*_L$	5.73 (0.002)
Thd	$n_{H-1}(O)\pi^*_L$	4.77 (0.010)	$n_{H-1}(O)\pi^*_L$	4.75 (0.006)
	$\pi_H\pi^*_L$	4.86 (0.193)	$\pi_H\pi^*_L$	4.82 (0.195)
	$\pi_H\sigma^*_{L+1}(CH_3)$	5.46 (0.004)	$\pi_H\sigma^*_{L+1}(CH_3)$	5.39 (0.004)
	$n_{H-3}(M)\pi^*_L$	5.83 (0.004)	$n_{H-3}(M)\pi^*_L$	5.79 (0.012)
Cyd	$\pi_H\pi^*_L$	4.65 (0.090)	$\pi_H\pi^*_L$	4.63 (0.092)
	$n_{H-1}(M)\pi^*_L - n_{H-2}(ON)\pi^*_L$[a]	4.84 (0.002)	$n_{H-1}(M)\pi^*_L - n_{H-2}(ON)\pi^*_L$[a]	4.83 (0.001)
	$n_{H-3}(N)\pi^*_L$	5.18 (0.002)	$\pi_H\sigma^*_{L+1}(NH_2)$	5.14 (0.005)
	$\pi_H\sigma^*_{L+1}(NH_2)$	5.21 (0.005)	$n_{H-3}(N)\pi^*_L$	5.19 (0.003)
Gud	$\pi_H\pi^*_L$	4.47 (0.016)	$\pi_H\pi^*_L$	4.41 (0.012)
	$\pi_H\pi^*_{L+1}$	4.74 (0.130)	$\pi_H\pi^*_{L+1}$	4.70 (0.119)
	$\pi_H\pi^*_{L+2}$	5.08 (0.121)	$\pi_H\pi^*_{L+2}$	5.02 (0.104)
	$\pi_H\pi^*_{L+3}$	5.15 (0.070)	$\pi_H\pi^*_{L+3}$	5.09 (0.084)

[a] A mixed nonbonding state with contributions from the ring O and N atoms as well as the ether O atom.

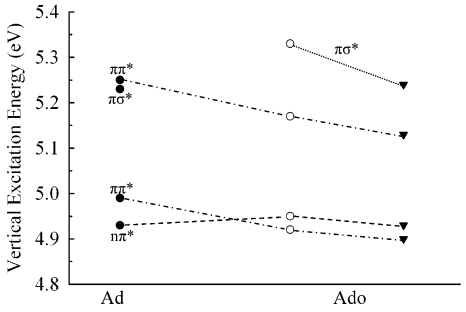

Figure 10. Vertical excitation energies of isolated adenine (Ad) and model ribose nucleoside (Ado). The "Add" model deoxyribose nucleotide compound does not optimize to a state analogous to the ribose nucleoside shown in Figure 1 and is not considered in the calculations. Correlations of excited state transitions are shown with lines. Calculations for Ado at the B3LYP/6-311++G(d,p) level are shown with open symbols, and those at the B3LYP/aug-cc-pVDZ level are shown with filled symbols. Further details of the nature of the transitions are given in Tables 2 and 3.

compounds, the purine N9−H9 and pyrimidine N1−H1 bonds are replaced by the "glycosidic" bond to the propyl group. The higher $n\pi^*$ transitions for the Xo species mix in contributions from the ether oxygen. The (*R*)-1-adenine-1-methoxypropane compound did not optimize to a structure compatible with the deoxyribose nucleoside and is not considered further.

Low-lying $\pi\sigma^*$ transitions are seen in the model deoxyribose-like pyrimidine derivatives. These $\pi\sigma^*$ transitions are localized on the methoxy group of the model sugar in uracil and thymine and on the NH_2 group in cytosine. The order and energy of the aromatic ring-localized $\pi\pi^*$ and $n\pi^*$ transitions in the deoxyribose analogues are similar to those in the free bases.

4. Discussion

The vertical excitation energies for isolated bases calculated with the TDDFT method at the B3LYP/6-311++G(d,p) and B3LYP/au-cc-pVDZ levels show good agreement with previous TDDFT results with comparable basis sets. Marian and coworkers have calculated vertical excitation energies for uracil[6] and adenine[9] at the DFT/MRCI level with large basis sets. The orbital assignments of the first four vertical excitations for uracil[6] are the same in the DFT/MRCI calculation as in the present work. However, the values of the vertical excitation energies for the second to fourth transitions determined from the DFT/MRCI calculations are higher than values calculated with TDDFT. The experimental range determined for the vertical excitation energy for the lowest lying $\pi\pi^*$ transition (4.6−5.1 eV) shows better agreement with the TDDFT calculations (5.13 eV) than the DFT/MRCI result (5.44 eV).

For adenine, the nature of the first vertical excitation is predicted differently by the TDDFT and DFT/MRCI calculations. The first two experimentally determined $\pi\pi^*$ vertical excitation energies for adenine are in the ranges of 4.3−4.6 and 4.6−4.9 eV, respectively.[2] The lower intensity 4.3−4.6 eV transition is predicted by the present calculations to be at 5.22 eV, while the DFT/MRCI calculations give a value of 4.90 eV for this transition. The more intense 4.6−4.9 eV transition is predicted by the present calculations to be at 4.95 eV, while the DFT/MRCI calculations give a value of 5.04 eV for this transition. The above comparisons show that the TDDFT method gives reasonable values for the vertical excitation energies when compared with experimental data. Further methodological developments for calculating excited electronic states will likely be required before uncertainties in the assignments and values for the vertical excitation energies can be further removed.

The results given in Tables 2 and 3 and Figures 6−10 show that the lowest lying excited states undergo qualitative and quantitative changes as a result of binding to molecules that model the sugar groups of nucleosides. To fully understand and accurately model the excited state relaxations in DNA, these changes would need to be considered.

Detailed mechanisms have been proposed for ultrafast decay of electronically excited adenine[9] from excited state levels determined from DFT/MRCI calculations and for cytosine[7] from excited state levels determined from CASPT2 calculations. In both calculations, conical intersections between low-lying $\pi\pi^*$ transitions and the S_0 state are responsible for the ultrafast internal conversion of the electronically excited bases. The nature and location of the conical intersections and radiationless decay mechanisms on the new excited state levels can be very different from those of the isolated bases. Figures 6−10 show that binding to the sugar analogues changes the energies of the low-lying levels. Whether these low-lying excited states in the nucleosides directly form conical intersections with the S_0 level or whether they first cross over with higher excited state remains to be determined by further calculations.

The results of fluorescence spectroscopy show that the S_1 ($0\rightarrow0'$) energy gaps of free bases, nucleosides, and nucleotides in solution are ordered as Ado ≥ Urd > Thd ≥ Cyd > Guo.[20] The calculated ordering of the vertical excitation energies of the isolated bases and model nucleosides in this work is

AdX > ThX > UrX ≥ CyX > GuX. The difference in ordering is expected since there will be changes in the relative energy of the electronic levels in going from the Franck−Condon structure to the S_1 state energy minimum.[6−11]

The model ethers of Figures 2 and 3 have structural similarities with the ribose and deoxyribose sugars shown in Figure 1. Although, in the ground electronic state, the acyclic ethers optimize to structures similar to the sugars and are appropriate for determining vertical excitation energies, the extra degrees of freedom of the ethers will lead to difficulties if structural optimizations for the excited states are attempted. Calculations of vertical excitation energies and excited state minima for the actual ribose and deoxyribose nucleosides or model furan-based ethers will eliminate this flexibility.[21]

An extension of the present calculations is to explicitly include water molecules in the excited state calculations. Solvent effects on the geometry and excitation energies of isolated bases have been studied theoretically by explicitly including water molecules in the electron structure calculations.[22−24] It is experimentally known that proton transfer from the solvent is not a rate-determining step in the decay of S_1 excited states in bases. Similar relaxation dynamics have been observed for adenine in water and acetonitrile and also in H_2O and D_2O.[25] Also, single and double proton transfer, specific solvent effects, and rare tautomeric forms are not considered to be important in the decay of the excited electronic states.[1] The equal relaxation times of bases in water and acetonitrile suggests that specific solvent/base interactions do not affect the nature of the relaxation dynamics. Polar solvents interact more strongly with nonbonded electrons in the ground state and lead to an increase in the energies (blue shift) of the nπ* transitions. The ground and excited levels for $\pi\pi$* transitions interact with the solvent to a roughly equal extent, and the energies of these transitions are less affected by solvation.

The effect of binding to complementary bases in the DNA molecule on the decay of excited electronic states is not considered in this work. Experimental studies show that the absorption spectra of multimers of given bases are not very different from the sum of spectra of the constituting monomers.[26] Most studies of base pair electronic excitations show that the excitations are localized on a single component of the pair.[1,4] These states will be perturbed by binding to sugar molecules and solvation.

Finally, the phosphate group is also observed to decrease the decay rate of pyrimidine nucleotides compared to the corresponding nucleosides, but this effect is not observed in purine bases.[27] The nonbonded electrons of the oxygen atoms can give rise to low-lying nπ* transitions. The effect of the phosphate group on the low-lying excitations remains to be deterimined.

5. Summary

The vertical excitation energies of model nucleoside compounds are calculated with the TDDFT method at the B3LPY/6-311++G(d,p) and B3LPY/aug-cc-pVDZ levels of theory. Ribose-like nucleoside model compounds with 1-methoxy-2-ethanol and deoxyribose-like nucleoside model compounds with 1-methoxypropane bound to purine and pyrimidine bases are studied. The first four vertical excitation energies for the isolated and water solvated molecules are determined.

Binding to the ethers causes qualitative and quantitative changes in the low-lying excited states. A small blue shift in nπ* states occurs upon binding of the base molecules to the ethers. Except in the case of adenine, where the nπ* and $\pi\pi$* states are closely spaced, binding to the ether alone does not lead to a reversal of the ordering of the first two excited states. Low-lying $\pi\sigma$* transitions from nitrogens at the N1 (pyrimidine) and N9 (purine) locations in the free bases are blue shifted as a result of binding to the ethers and formation of N−C bonds. New $\pi\sigma$* transitions are introduced in the low-lying states as a result of binding to the ether molecules. Except for the case of cytosine, these new transitions originate from the ether molecules. The new transitions and the change of spacing of the $\pi\pi$* and nπ* states may have considerable effects on the electronic deexcitation rates and mechanisms.

References and Notes

(1) Crespo-Hernández; Cohen, B.; Hare, P. M.; Kohler, B. *Chem. Rev.* **2004**, *104*, 1977.
(2) Shukla, M. K.; Leszczynski, *J. Comput. Chem.* **2004**, *25*, 768.
(3) Salter, L. M.; Chaban, G. M. *J. Phys. Chem. A* **2002**, *106*, 4251.
(4) Zhanpeisov, N. U.; Leszczynski, J. *J. Phys. Chem. A* **1998**, *102*, 6167.
(5) Ismail, N.; Blancafort, L.; Olivucci, M.; Kohler, B.; Robb, M. A. *J. Am. Chem. Soc.* **2002**, *124*, 6818.
(6) Marian, C. M.; Schneider, F.; Kleinschmidt, M.; Tatchen, J. *Eur. Phys. J. D* **2002**, *20*, 357.
(7) Merchán, M.; Serrano-Andés, L. *J. Am. Chem. Soc.* **2003**, *125*, 8108.
(8) Sobolewski, A. J.; Domcke, W. *Phys. Chem. Chem. Phys.* **2004**, *6*, 2763.
(9) Marian, C. M. *J. Chem. Phys.* **2005**, *122*, 103414.
(10) Sobolewski, A. J.; Domcke, W. *Eur. Phys. J. D* **2002**, *20*, 369.
(11) Zhang, L.; Peritz, A.; Meggers, E. *J. Am. Chem. Soc.* **2005**, *127*, 4174.
(12) Frisch, M. J.; Trucks, G. W.; Schlegel, H. B.; Scuseria, G. E.; Robb, M. A.; Cheeseman, J. R.; Zakrzewski, V. G.; Montgomery, J. A., Jr.; Stratmann, R. E.; Burant, J. C.; Dapprich, S.; Millam, J. M.; Daniels, A. D.; Kudin, K. N.; Strain, M. C.; Farkas, O.; Tomasi, J.; Barone, V.; Cossi, M.; Cammi, R.; Mennucci, B.; Pomelli, C.; Adamo, C.; Clifford, S.; Ochterski, J.; Petersson, G. A.; Ayala, P. Y.; Cui, Q.; Morokuma, K.; Salvador, P.; Dannenberg, J. J.; Malick, D. K.; Rabuck, A. D.; Raghavachari, K.; Foresman, J. B.; Cioslowski, J.; Ortiz, J. V.; Baboul, A. G.; Stefanov, B. B.; Liu, G.; Liashenko, A.; Piskorz, P.; Komaromi, I.; Gomperts, R.; Martin, R. L.; Fox, D. J.; Keith, T.; Al-Laham, M. A.; Peng, C. Y.; Nanayakkara, A.; Challacombe, M.; Gill, P. M. W.; Johnson, B.; Chen, W.; Wong, M. W.; Andres, J. L.; Gonzalez, C.; Head-Gordon, M.; Replogle, E. S.; Pople, J. A. *Gaussian 98*, revision A.7; Gaussian, Inc.: Pittsburgh, PA, 2001.
(13) (a) Parr, R. G.; Yang, W. *Density Functional Theory of Atoms and Molecules*; Oxford University Press: New York, 1989. (b) Koch, W.; Holthausen, M. C. *A Chemists View of Density Functional Theory*; Wiley-VCH: Weinheim, Germany, 2000.
(14) Becke, A. D. *J. Chem. Phys.* **1993**, *98*, 5648.
(15) Lee, C.; Yang, W.; Parr, R. G. *Phys. Rev. B* **1988**, *37*, 785.
(16) Casida, M. E.; Jamorski, C.; Casida, K. C.; Salahub, D. R. *J. Chem. Phys.* **1998**, *108*, 4439.
(17) Stratmann, R. E.; Scuseria, G. E.; Frisch, M. J. *J. Chem. Phys.* **1998**, *109*, 8218.
(18) Dunning, T. H., Jr. *J. Chem. Phys.* **1990**, *90*, 1007.
(19) Woon, D. E.; Dunning, T. H., Jr. *J. Chem. Phys.* **1993**, *98*, 1358. Peterson, K. A.; Woon, D. E.; Dunning, T. H., Jr. *J. Chem. Phys.* **1994**, *100*, 7410.
(20) Cadet, J.; Vigny, P. In *Bioorganic Photochemistry*; Morrison, H., Ed.; Wiley: New York, 1990; Vol. 1, p 1.
(21) Alavi, S. Unpublished work.
(22) Broo, A.; Holmén, A. *J. Phys. Chem. A* **1997**, *101*, 3589.
(23) Shukla, M. K.; Mishra, S. K.; Kumar, A.; Mishra, P. C. *J. Comput. Chem.* **2000**, *21*, 826.
(24) Shukla, M. K.; Leszczynski, J. *J. Phys. Chem. A* **2002**, *106*, 8642.
(25) Cohen, B.; Hare, P. M.; Kohler, B. *J. Am. Chem. Soc.* **2003**, *125*, 13594.
(26) Eisinger, J.; Shulman, R. G. *Science* **1968**, *161*, 1311.
(27) Onidas, D.; Markovitsi, D.; Marguet, S.; Sharanov, A.; Gustavsson, T. *J. Phys. Chem. B* **2002**, *106*, 11367.